Effects of post-annealing treatment on the structure and photoluminescence properties of CdS/PS nanocomposites prepared by sol-gel method*

ZHANG Hong-yan (张红燕)**
School of Physical Science and Technology, Xinjiang University, Urumqi 830046, China

(Received 30 November 2015)

CdS nanocrystals have been successfully grown on porous silicon (PS) by sol-gel method. The plan-view field emission scanning electron microscopy (FESEM) shows that the pore size of PS is smaller than 5 μm in diameter and the agglomerates of CdS are broadly distributed on the surface of PS substrate. With the increase of annealing time, the CdS nanoparticles grow in both length and diameter along the preferred orientation. The cross-sectional FESEM images of ZnO/PS show that CdS nanocrystals are uniformly penetrated into all PS layers and adhere to them very well. photoluminescence (PL) spectra demonstrate that the intensity of PL peak located at about 425 nm has almost no change after the annealing time increases. The range of emission wavelength of CdS/PS is from 425 nm to 455 nm and the PL intensity is decreasing with the annealing temperature increasing from 100 °C to 200 °C.
Document code: A **Article ID:** 1673-1905(2016)02-0081-4
DOI 10.1007/s11801-016-5240-1

Over the last decade, stable and high luminescence CdS nanocrystals have been synthesized by means of physical vapor deposition (PVD), chemical bath deposition (CBD), electrochemical reaction, solvothermal methods, sol-gel method and organometallic synthesis, etc[1-3]. Among these methods, the sol-gel method attracts increasing interest because of its simplicity, safety, large area coating capability, low cost and low deposition temperature. The use of nanoparticles will lead to a low light scattering and high transparency of the coatings[4]. CdS nanostructures grown on Si-based substrates have received significant attention. However, it is difficult to directly grow or deposite high quality CdS nanostructures on silicon substrates, because there is a large stress between CdS and Si substrate due to the mismatch in their thermal expansion coefficients and lattice constants.

In the early stages of the research on porous silicon (PS)-based applications, the focus was mainly on the development of optoelectronic devices, such as light emitting diodes (LEDs) and solar cells[5-7]. Several reports suggested that the porous layer is a good substrate in lattice mismatch heteroepitaxy because of its special surface morphology[8-10].

In this study, CdS/PS nanocomposites have been successfully synthesized via sol-gel method, and such prepared CdS/PS nanocomposites show much higher and more stable activity for photoluminescence (PL) properties. Studies of the thermal annealing effects on microstructure properties of CdS/PS nanocomposites are conducted. The CdS nanoparticles grown on PS substrate will pave the way for integration of CdS-based devices with current Si-based IC technology.

All chemicals utilized in this study are of analytical grade and they were used without any further purification. PL spectra were measured by the excitation of Xe lamp (Hitachi, F-4600, Japan) with the excitation wavelength of 370 nm, and all spectra were measured at room temperature. Surface and cross-sectional images were obtained by a field emission scanning electron microscope (FESEM) (Hitachi, S4800, Japan).

The Si substrates used in this study are n-type, 1—10 Ω·cm resistivity, (100) orientation, and 420 ±15 μm thick. The substrates were cut into squares and cleaned with the solution of acetone, alcohol and deionized water. Then the substrates were placed in a teflon electrochemical etch cell using a piece of Cu as the counter electrode, with an area of approximately 0.2 cm^2 exposed to the solution. The cell was filled with a 1:3 (volume ratio) mixture of 48% HF and absolute ethanol. The anodic current density is 50 mA/cm^2 for 20 min and the etching process was performed at 55 °C. After being etched, the prepared fresh PS was soaked into H_2O_2 (30%) for 24 h at room temperature. Then the substrates were rinsed with deionized water and dried in the air.

In the typical synthesis, 0.036 6 g calcium chloride ($CaCl_2$), 0.07 g sodium thiosulfate pentahydrate ($Na_2S_2O_3·5H_2O$) and 0.074 g sodium citrate ($Na_3C_6H_5O_7$)

* This work has been supported by the Xinjiang Science and Technology Project (No.2015211C275).
** E-mail: zhanghongyanxj@163.com

were dissolved in 200 mL deionized water. The resulting mixture was stirred thoroughly by a magnetic stirrer for 15 min, and then 0.2 g sodium borohydride ($NaBH_4$) was added and stirred for 10 min. After complete homogenization, 0.044 g L-cysteine ($C_3H_7NO_2S$) was added to the mixture and stirred for 30 min until a yellow and clear solution was obtained. Then the above solution and oxidized PS were kept in a teflon-line autoclave with 200 mL capacity, and maintained constantly at different temperatures for different time in an oven. In the fabrication, $CdCl_2$ and 0.07 g $Na_2S_2O_3 \cdot 5H_2O$ were used as the precursors for Cd and S, respectively.

Fig.1 shows the FESEM images of the CdS/PS nanocomposites annealed at 180 °C with annealing time of 40 min, 60 min and 80 min. Fig.1(a) shows that the agglomerates of CdS are broadly distributed on the surface of PS substrate. Fig.1(b) shows that the CdS nanocrystals consist of small crystals in a perfectly aligned manner with a size about 20 nm and spherically shaped morphology when annealed for 40 min. With the annealing time increasing to 80 min, the size of agglomerates of CdS increases to 1 μm and the morphology of CdS nanocrystals becomes flower-like shape. From the SEM images, it can be seen that the annealing time can affect the diameter and shape of CdS nanocrystals. With the annealing time increasing, the CdS nanoparticles grow in diameter along a preferred orientation.

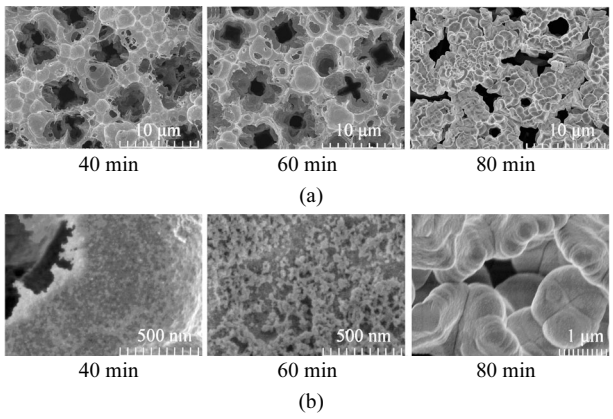

Fig.1 (a) Plan-view FESEM images of CdS/PS nanocomposites annealed at 180 °C with different annealing time; (b) High resolution plan-view FESEM images of ZnO/PS nanocomposites corresponding to (a)

The main results in this work are the analyses of PL emission of ZnO/PS nanocomposites in the visible region with different post-annealing treatments. Fig.2 shows the PL spectra of CdS/PS nanocomposites annealed at 180 °C with different annealing time, where the excitation wavelength is 370 nm and the PL peak is located at about 425 nm. Generally in semiconductor nanomaterials, the various mechanisms contributing to the PL emission include band edge emission, deep trap emission, surface defect emission and the nanoparticle size distribution[11]. For CdS nanoparticles, there are four types of point defects: interstitial cadmium (I_{Ca}), interstitial sulfur (I_s), cadmium vacancy (V_{Ca}) and sulfur vacancy (V_s), and they play an important role for PL spectra[12]. The emission spectrum of CdS/PS nanoparticles demonstrates a blue emission around 425 nm (UV band). The peak may correspond to the near band edge emission in the wide band gap of CdS. It can be seen that the peak intensity of CdS/PS nanocomposites has almost no change as the annealing time increases from 40 min to 80 min. Taking all the measurement into consideration, we can conclude that the annealing temperature has slight influence on the PL intensity of CdS/PS nanocomposites.

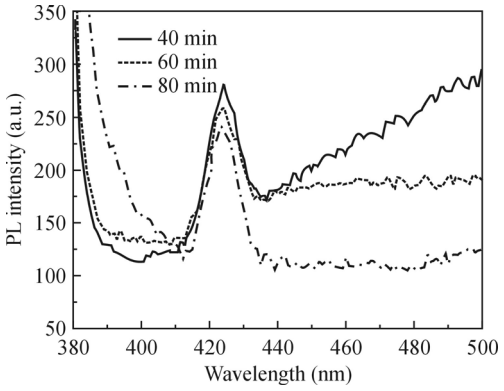

Fig.2 Room-temperature PL spectra (λ_{exc}=370 nm) of CdS/PS nanocomposites annealed at 180 °C with different annealing time

Fig.3 shows the PL spectra of CdS/PS nanocomposites with different annealing temperatures for 40 min. The PL spectra were recorded at 325 nm excitation and a broad visible light beam was emitted from approximately 400 nm to 500 nm, where a strong PL emission peak is at approximately 425 nm. The peak may correspond to the near band edge emission in the wide band gap of CdS[3,13], which results from the direct recombination of photo-generated charge carriers and surface defects localized exciton and intrinsic exciton. The emission peak with minor humps indicates that there is a quantum confinement effect. In Fig.3(b), it can be clearly seen that the PL emission peak of CdS shifts from 425 nm to 455 nm with the increase of the annealing temperature. Such a Stokes shift is ascribed to the surface states or defects[14]. In general, the larger the Stokes shift, the larger the concentration of surface state or defect. Thus the PL spectra are dominated by a strong and narrow band edge emission tunable in the blue region of the visible spectrum, indicating a narrow distribution of CdS nanocrystals. This band edge is possibly comprised of the recombination of luminescence of shallow traps or surface defects localized exciton and intrinsic excition. Furthermore, the intensity of UV emission decreases with the increase of annealing temperature, which indicates that the improvement of the crystallinity of CdS nanoparticles results from free exciton emission. We can conclude that the annealing temperature plays a crucial role in the formation of CdS/PS nanocomposites with various crystal

structures, shapes and sizes. Taking all the measurement into consideration, the annealing temperature of 100 °C is of high crystallinity with fewer defects.

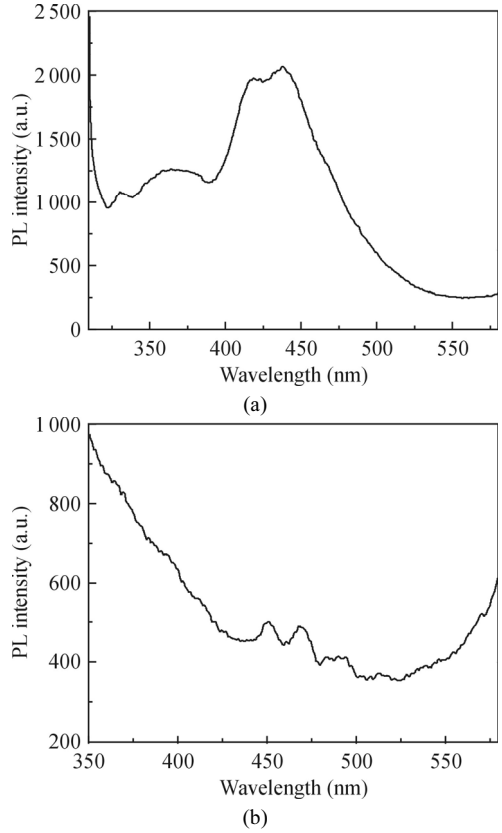

Fig.3 Room-temperature PL spectra (λ_{exc}=325 nm) of CdS/PS nanocomposites annealed for 40 min with different annealing temperatures: (a) 100 °C and (b) 200 °C

Fig.4(a) shows the plan-view FESEM image of CdS/PS nanocomposites annealed at 100 °C for 40 min. The CdS nanocrystals were grown on PS layer with sponge-like porous structure, where the pore size of PS is usually less than 5 μm in diameter, which facilitates sufficient mass transport characteristics for loading CdS sol. In the fabrication of CdS/PS nanocomposites, porous layer acts not only as a good substrate to reduce lattice mismatch, but also as a nucleation site to induce the CdS nanoparticles to grow along the same orientation as the porous layer. In Fig.4(b), the CdS nanoparticles are packed regularly and appear as homogeneous granules. The size of CdS nanocrystals is about 20 nm with sphere-shaped morphology. Fig.4(c) shows the cross-sectional FESEM image of PS substrate after CdS nanoparticles were deposited on it, where the overall thickness of PS is approximately 12 μm, and these macro-pores contain smaller nano-dimensional pores. The pore size is large enough to permit CdS sol to infiltrate into PS substrate, and CdS nanocrystals are uniformly penetrated into all PS layers and adhere to them very well.

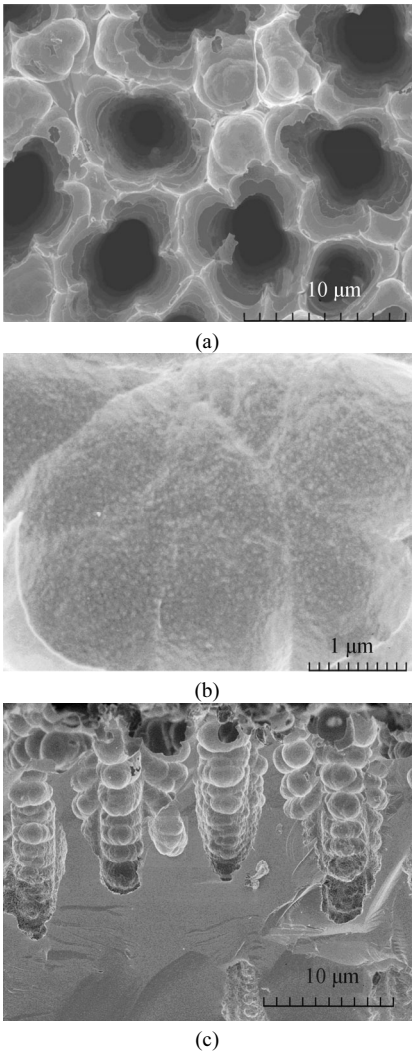

Fig.4 (a) Plan-view FESEM image of CdS/PS nanocomposites annealed at 100 ºC for 40 min; (b) High resolution plan-view FESEM image of ZnO/PS nanocomposites corresponding to (a); (c) Cross-sectional FESEM image of ZnO/PS nanocomposites corresponding to (a)

In summary, CdS/PS nanocomposites have been directly synthesized by sol-gel method. The structural, surface morphological investigation from FESEM and optical PL spectra reveal that the formation of high CdS yields nanocrystals. The analysis of FESEM shows that the CdS nanoparticles grow in diameter with the annealing temperature increasing along with an increasingly preferred orientation. The PL spectra demonstrate that the PL peak is located at about 425 nm and the PL intensity has almost no change when the annealing time increases. Moreover, the tuning range of emission wavelength is from 425 nm to 455 nm, and the PL intensity decreases with the annealing temperature increasing. We can conclude that the annealing time has slight influence on the PL intensity of CdS/PS nanocomposites. But the annealing temperature plays a crucial role in the PL intensity of CdS/PS nanocomposites. With good optical properties, this simple synthesis method of CdS/PS nanocomposites has a potential application in the inte-

gration of future UV optoelectronic devices.

References

[1] A. Salavei, I. Rimmaudo, F. Piccinelli, P. Zabierowski and A. Romeo, Solar Energy Materials and Solar Cells **112**, 190 (2013).

[2] A. Mukherjee, M. Fu, P. Ghosh and P. Mitra, Materials Letters **141**, 39 (2015).

[3] B. Ren, M. Cao, Q. Zhang, J. Huang, Zhi Zhao, Xiang Jin, Chao Li, Yue Shen and Linjun Wang, Journal of Alloys and Compounds **659**, 74 (2016).

[4] L. B. Duan, X. R. Zhao, Y. J. Wang, H. Shen, W. C. Geng and F. L. Zhang, Journal of Alloys and Compounds **645**, 529 (2015).

[5] H. Ma and H. Y. Zhang, Optoelectronics Letters **11**, 95 (2015).

[6] YAN Pei-qin, LI Zhao-hui, SHI Ya-fan, FENG Bai-cheng, DU Bing-cheng, DU Yan-wei, TAN Tian-le and WU Guang, Optoelectronics Letters **11**, 321 (2015).

[7] L.T. Canham, Appl. Phys. Lett. **57**, 1046 (1990).

[8] Hsuan-Chih Chu, Tzung-Chi Liang, Harihara Padhy, Shou-Jen Hsu and Hong-Cheu Lin, European Polymer Journal **47**, 2266 (2011).

[9] B. Mahmoudi, N. Gabouze, L. Guerbous, M. Haddadi and K. Beldjilali, Journal of Luminescence **127**, 534 (2007).

[10] H.Y. Zhang, X.Y. Lv, C.W. Lv and Z.H. Jia, Optical Engineering **51**, 099003 (2012).

[11] F. Antolini, E. Burresi, L. Stroea, V. Morandi, L. Ortolani, G. Accorsi and M. Blosi, Journal of Nanaomaterials **2012**, 1 (2012).

[12] S. K. Tripathi, R. Kaur and J. Kaushal, Optics Communications **352**, 55 (2015).

[13] J. S. Roy, T. P. Majumder and C. Schick, Journal of Molecular Structure **1088**, 95 (2015).

[14] A. E. Ragab, A. S. Gadallah, M. B. Mohamed and I. M. Azzouz, Optics Laser Technology **63**, 8 (2014).